THE INFLUENCE OF EQUILIBRIUM REACTIONS ON THE KINETICS OF CALCITE DISSOLUTION IN LACTIC ACID SOLUTIONS

A Thesis

by

DANIEL COLLIER SHEDD

Submitted to the Office of Graduate and Professional Studies of
Texas A&M University
in partial fulfillment of the requirements for the degree of

MASTER OF SCIENCE

Chair of Committee,	Hisham A. Nasr-El-Din
Committee Members,	Robert H. Lane
	Mahmoud El-Halwagi
Head of Department,	A. Daniel Hill

August 2014

Major Subject: Petroleum Engineering

ABSTRACT

Matrix acidizing has historically been a common means of removing formation damage and increasing the productivity of petroleum wells. Organic acids have been used in an effort to minimize the corrosion problem and the rapid reaction rate encountered when using strong acids, such as hydrochloric acid (HCl). The reaction of an organic acid with carbonates is reversible and thermodynamically limited by the presence of reaction products. This thermodynamic limitation must be considered when studying the reaction kinetics of organic acids with carbonates.

A kinetic model was developed to account for both the equilibrium reactions on the rock surface and the mass transfer of the reactants and products. This study provides both mass transport and reaction kinetics parameters, which can be combined with the reservoir temperature to determine treatment duration or soaking time. While lactic acid has been used successfully in the field, having a more detailed knowledge of the reaction between lactic acid and calcite will allow for optimized treatment design.

The kinetic model was also used to isolate the contributions of the transport of reactants, the surface reaction, and the transport of products to the overall resistance of the reaction. At all temperatures investigated, the transport of products away from the surface represented the largest contribution to overall resistance.

A coreflood experiment was also performed to observe and confirm the wormholing tendencies of lactic acid in calcite. Lactic acid formed a single dominant, minimally-branched wormhole through the core.

ACKNOWLEDGEMENTS

I would like to thank my committee chair, Dr. Nasr-El-Din, for his guidance and for providing me with the opportunity to further my education and learning. I would also like to thank Dr. Lane and Dr. El-Halwagi for serving on my committee.

My friends and colleagues also deserve thanks for their encouragement in times of frustration and for making my time at Texas A&M University an enjoyable one.

Finally, I would like to thank my parents for their constant support and encouragement.

NOMENCLATURE

D	diffusion coefficient
E_a	activation energy
HCl	hydrochloric acid
HL	lactic acid
I	ionic strength
ICP-OES	inductively coupled plasma-optical emission spectroscopy
k_b	backward reaction rate constant
K_c	conditional equilibrium constant
K_{eff}	effective equilibrium constant
k_f	forward reaction rate constant
K_{MT}	mass transfer coefficient
k_r	effective surface reaction rate constant
L	lactate ion
n	reaction order
r_D	dissolution rate
RDA	rotating disk apparatus
r_s	surface reaction rate
Sc	Schmidt number
T	temperature
z	ionic charge

γ	activity coefficient
κ	overall reaction rate constant
ν	kinematic viscosity
ω	disk rotational speed

TABLE OF CONTENTS

Page

ABSTRACT ii

ACKNOWLEDGEMENTS iii

NOMENCLATURE iv

TABLE OF CONTENTS vi

LIST OF FIGURES vii

LIST OF TABLES viii

CHAPTER I INTRODUCTION AND LITERATURE REVIEW 1

CHAPTER II THE ROTATING DISK APPARATUS 6

CHAPTER III KINETIC MODEL 9

Chatelain et al. Model 9
Buijse et al. Model 10

CHAPTER IV EXPERIMENTAL RESULTS AND ANALYSIS 21

Mass Transfer Study – Reaction of Lactic Acid with Calcite 22
Kinetic Study – Reaction of Lactic Acid with Calcite 25

CHAPTER V COREFLOOD INVESTIGATION 33

CHAPTER VI APPLICATION AND CONCLUSIONS 39

CHAPTER VII FUTURE WORK 42

REFERENCES 43

APPENDIX SUMMARY OF EXPERIMENTAL DATA 47

LIST OF FIGURES

Page

Figure 3.1 – Reaction of 5 wt% lactic acid with Indiana limestone from 80-250°F.....15

Figure 3.2 – Reaction of 5 wt% lactic acid with Indiana limestone at 200°F.....15

Figure 3.3 – Kinematic viscosity of 5 wt% lactic acid as a function of temperature.....17

Figure 4.2 – Calculated diffusion coefficients of 5 wt% lactic acid versus temperature.....24

Figure 4.3 – Comparison of estimated and calculated diffusion coefficient values.....25

Figure 4.4 – Reciprocal dissolution rate versus reciprocal of the square root of rotational speed for 5 wt% lactic acid at 80, 150, and 250°F.....28

Figure 4.5 – Comparison of experimental and model K_{eff} values and k_r. 30

Figure 4.6 – Effect of Temperature on Kinetics.....31

Figure 5.1 – Schematic of coreflood apparatus.....33

Figure 5.2 – Pressure drop data during acid injection.....35

Figure 5.3 – CT scan image of core after acid injection. 36

Figure 5.4 – The effect of injection rate on wormhole geometry.....37

LIST OF TABLES

Page

Table 3.1 – Kinematic viscosity (cm^2/sec) of 5 wt% lactic acid. 16

Table 3.2 – Diffusion coefficients (cm^2/s) used in model calculations. 18

Table 3.3 – Equilibrium reactions for calcite/lactic acid system and corresponding equilibrium constants at 25°C 18

Table 3.4 – Values of A and B constants for water 19

Table 3.5 – Values of a and b parameters for each ionic species. 20

Table 3.6 – Effective equilibrium constants calculated from model. 20

Table 4.1 – Reaction kinetics and mass transfer properties of lactic acid with Indiana limestone from 80-250°F. 29

Table 4.2 – Effect of reversible reaction on calculation of reaction rate constant. 32

CHAPTER I

INTRODUCTION AND LITERATURE REVIEW

Matrix acidizing has historically been a common means of removing formation damage and increasing the productivity of petroleum wells. First patented in 1896, matrix acidizing began when the Standard Oil Company stimulated carbonate formations with concentrated hydrochloric acid (Kalfayan 2008). Even during these first acidizing treatments, it was acknowledged that the direct contact of HCl with well components could cause major corrosion problems.

The goal of matrix acidizing in carbonates is the formation of long wormholes that penetrate deep into the formation, either bypassing near-wellbore formation damage or enhancing the flow capacity of the near-wellbore area in undamaged formations. Formation damage is "the impairment of the permeability of petroleum-bearing formations by various adverse processes" (Civan 2007). This damage can occur through seven different mechanisms which are common to both horizontal and vertical wells: fluid-fluid incompatibilities, rock-fluid incompatibilities, solids invasion, phase trapping/blocking, chemical adsorption/wettability alteration, fines migration, or biological activity (Bennion and Thomas 1994). While matrix acidizing cannot be used to mitigate all forms of formation damage, it is a useful technique used to remove acid-soluble damaging material.

The dissolution of calcium carbonate, or calcite, in acids has been extensively studied for many years (Lund, Fogler, and McCune 1973; Lund et al. 1975; Plummer,

Wigley, and Parkhurst 1978; Pokrovsky, Golubev, and Schott 2005; Pokrovsky et al. 2009; Sjöberg and Rickard 1984). The heterogeneous overall reaction that occurs between acidic fluids and calcite consists of three potential surface reactions. Calcite can be dissolved by the hydrogen ion, by carbonic acid, or by water via the following three reactions:

$$H^+ + CaCO_3 \rightleftharpoons Ca^{2+} + HCO_3^- \quad 1.1$$

$$H_2CO_3 + CaCO_3 \rightleftharpoons Ca^{2+} + 2HCO_3^- \quad 1.2$$

$$H_2O + CaCO_3 \rightleftharpoons Ca^{2+} + HCO_3^- + OH^- \quad 1.3$$

Eq. 1.1 dominates when the pH is low. Eq. 1.2 is only significant when the partial pressure of CO_2 is greater than 0.1 atm and the pH is greater than 5.0. Eq. 1.3 is the dominant reaction at high pH. Since the reactions of interest to acidizing treatments occur at reservoir pressure and low pH, Eq. 1.1 will be the dominant reaction.

Hydrochloric acid (HCl) has been used very frequently in matrix acidizing treatments. HCl is a strong, inexpensive acid which spends very rapidly upon contact with carbonate formations. At low to moderate temperatures, HCl treatments can be very effective in many different environments. As technology continues to advance, wells are being drilled deeper and deeper, which can result in very high bottomhole temperatures. In these cases, the reaction rate of HCl with carbonate formations becomes very rapid. This can lead to uniform dissolution around the wellbore, which has a very minimal effect in restoring or enhancing near-wellbore permeability, and potentially the collapse of weakly consolidated formations.

The corrosion of metallic components is another major concern when designing acid treatments, especially at elevated temperatures. The corrosion rate depends greatly on "the susceptibility of the material under the environmental conditions to which it is exposed" (Tuttle 1987). In order to minimize the corrosion rate, corrosion inhibitors are added to the acid solution before the treatment is pumped. Film-forming amines and their salts are typically the most effective type of corrosion inhibitors, but these begin to decompose at 482°F (Schauhoff and Kissel 2000). Also, acid corrosion inhibitors can have potentially damaging effects on stimulation results due to the inhibitor being adsorbed into the formation, which can result in altered wettability or severe emulsion problems (Crowe and Minor 1985). As the environment becomes more extreme (higher temperature or less corrosion-resistant metallurgy), a higher loading of corrosion inhibitor or inhibitor intensifiers become necessary. These inhibitors, when combined with the other additives present in the treatment fluid, can result in fluid compatibility issues. Organic acids, with their lower corrosivity and slower reaction rates, have the potential to counteract both of the major issues encountered when using HCl in extreme environments.

Organic acids have been used in an effort to minimize the corrosion problem and the rapid reaction rate encountered when using strong acids. Organic acids are weakly-ionized, slow-reacting, and have less dissolving power than HCl, meaning they are more expensive per unit volume of rock dissolved when compared to HCl (Li et al. 2008; Al-Khaldi et al. 2005). Organic acids cannot be used in high concentrations due to the limited solubility of their corresponding calcium salts. In addition, the reaction of an

organic acid with carbonates is reversible and thermodynamically limited by the presence of reaction products (Al-Khaldi et al. 2005). A significant advantage of lactic acid over other organic acids is its increased solubility at high temperature. The solubility of calcium lactate has been shown to be nearly 50 g anhydrous calcium lactate per 100 g of solution at 176°F (Kubantseva and Hartel 2002).

Lactic acid is an α-hydroxy acid with a chemical formula of $C_3H_6O_3$ and a molecular weight of 90.08. Previous oilfield applications include acid fracturing, iron control agent, and filter cake removal (Rabie and Nasr-El-Din 2011). It is similar in strength to formic acid, and has a dissociation constant approximately ten times greater than acetic acid (Al-Otaibi, Al-Moajil, and Nasr-El-Din 2006). Due to these similarities and advantages, the potential of lactic acid as a standalone stimulation fluid was investigated.

The purpose of carbonate matrix acidizing is to form wormholes that penetrate into the formation and past the damaged zone. The factors that control optimal wormholing are the surface reaction rate between the stimulation fluid and the formation and the mass transfer of the stimulation fluid (Huang, Hill, and Schechter 2000). The reaction of an organic acid with carbonate minerals consists of three distinct steps: the transport of reactants from the bulk solution to the mineral surface, the reaction of the acid on the mineral surface, and the transport of products away from the surface back to the bulk solution. Before lactic acid can be considered as a standalone stimulation fluid, these three steps must be isolated and investigated independently, which will allow for wormholing to be optimized using the surface reaction rate and the mass transfer of the

stimulation fluid. This study presents the first in-depth kinetic analysis of the lactic acid-calcite reaction. A kinetic model was developed to account for both the equilibrium reactions on the rock surface and the mass transfer of the reactants and products. This study provides both mass transport and reaction kinetics parameters, which can be combined with the reservoir temperature to determine treatment duration or soaking time. While lactic acid has been used successfully in the field, having a more detailed knowledge of the reaction between lactic acid and calcite will allow for optimized treatment design.

Dissolution rate values were obtained from experiments using the rotating disk reactor, which is described in the next chapter. These experiments were performed by Ahmed Rabie (Rabie and Nasr-El-Din 2011), and were compiled for submission to a SPE Journal. It was determined by the reviewers that the analysis was innately flawed, so the initial submission was rejected. A more thorough analysis was deemed necessary, and the work included in this thesis was in response to editor comments. After this analysis was applied to the experimental data, the paper was accepted for publication.

CHAPTER II

THE ROTATING DISK APPARATUS

The rotating disk apparatus (RDA) is commonly used in the oil industry to determine the reaction rate between a fluid and a reactive rock sample. This system possesses distinct advantages over flat plate systems as presented by Boomer et al. (Boomer, McCune, and Fogler 1972). First, the rotation of the disk induces the flow of the liquid, negating the necessity of a flow tunnel. Secondly, this system does not require large fluid volumes. End effects are also minor with a rotating disk, whereas they can be a major consideration in flat plate flow systems. End effects are considered negligible when boundary layer thickness is small compared to disk radius, and the thickness of this layer is constant over the entire disk surface (Levich 1962). For laminar flow at the surface of a rotating disk in an infinite fluid volume, an exact solution of the Navier-Stokes equations exists. Laminar flow at the surface of a rotating disk exists below a Reynolds number ($Re = \omega R^2/\upsilon$) of approximately 2.5 x 10^5 (Ellison and Cornet 1971). In this study, this Reynolds number corresponds to a maximum rotational speed of approximately 1880 rpm at 250°F where the kinematic viscosity will be lowest. All experiments were conducted below this maximum rotational speed. For a Reynolds number of approximately 10, the thickness of the hydrodynamic boundary layer becomes comparable to the radius of the disk (Levich 1962). A Reynolds number of 10 corresponds to a rotational speed of approximately 0.25 RPM at 80°F, where kinematic

viscosity will be highest. Finally, the surface of a rotating disk is uniformly accessible, meaning there are no radial temperature or concentration gradients.

The flux of solute, J, is given as (Newman 1966):

$$J = \left[\frac{0.62048\, Sc^{-2/3}\sqrt{\upsilon\omega}}{0.2980\, Sc^{-1/3} + 0.1451\, Sc^{-2/3}}\right](C_b - C_i) \qquad 2.1$$

where the bracketed terms represent the mass transfer coefficient, Sc is the Schmidt number ($Sc = \upsilon/D$), ν is the kinematic viscosity, D is the diffusion coefficient, ω is the disk rotational speed, and C_b and C_i are the bulk and interface concentrations respectively.

The rotating disk apparatus used in the scope of this project was a CRS-1000 Rotating Disc Acid Reaction System obtained from Core Laboratories. The stimulation fluid is loaded into a Hastelloy B pre-charge cell, and the reactive rock sample is attached to a magnetic drive system with heat shrink Teflon tubing and loaded into the Hastelloy B primary cell. Heating jackets on both cells are used to raise the temperature of the cells and the stimulation fluid to the desired experimental temperature, up to 250°F. Once that temperature is reached, the stimulation fluid is displaced into the primary measurement cell by gas drive and the experimental timer is started. Once this displacement has occurred, the measurement cell is pressurized to the desired pressure, up to 3,000 psi. In order to keep any generated CO_2 in solution, a pressure of at least 800 psi was maintained. Failure to keep the generated CO_2 in solution can affect the reaction of organic acids with carbonate and can disrupt the laminar flow on the surface of the disk due to the formation of bubbles (Taylor and Nasr-El-Din 2009). After the

measurement cell is pressurized, the magnetic drive system is set to the desired rotation speed, from 100 to 1800 rpm. Samples are withdrawn periodically, where the precise time intervals depend upon both the fluid and the rock type being used. The ion composition of these samples is measured using a Perkin Elmer Optima 7000 DV ICP-OES after being diluted to a concentration within the measurable range of the ICP equipment. The dissolution rate is then calculated based on the increase of calcium concentration in the samples with respect to time. This value is also corrected using the surface area of the disk.

CHAPTER III

KINETIC MODEL

The reversible reaction that occurs between organic acids and carbonate minerals is a well-known phenomenon. Hydrochloric acid is used in part due to its complete dissociation, which allows the reaction to proceed to completion. Since organic acids do not dissociate completely, it is important to account for this thermodynamic limitation on the reaction. The work of Chatelain et al., and Buijse et al. are two of the more prominent publications regarding the use of organic acids in carbonate acidizing (Buijse et al. 2004; Chatelain, Silberberg, and Schechter 1976).

Chatelain et al. Model

First, the Chatelain et al. Model represents a thermodynamic approach in modeling the reaction of an organic acid with carbonates (Chatelain, Silberberg, and Schechter 1976). Presenting only the final result of the analysis present in the paper, the following two equations are used:

$$K_3\left(\frac{\gamma_{HA}\gamma_{Ca^{2+}A^-}^{3/2}}{\gamma_{CaA^+A^-}^{2}\gamma_{CO_2}^{1/2}}\right)=\frac{\left[\frac{1}{2}\mathrm{X}\beta-(Ca^{2+})\right]\left(\frac{1}{2}\mathrm{X}\beta\right)^{1/2}}{K_1^{1/2}K_2(N-\mathrm{X})\beta(Ca^{2+})^{1/2}} \tag{3.1}$$

and

$$\left(\frac{\gamma_{HA}}{\gamma_{Ca^{2+}A^-}^{3/2}\lambda_{CO_2}^{1/2}}\right)\cdot\frac{K_1^{1/2}K_2(N-\mathrm{X})\beta}{\left(\frac{1}{2}\mathrm{X}\beta\right)^{1/2}(Ca^{2+})^{1/2}}-(Ca^{2+})=\frac{1}{2}\mathrm{X}\beta \tag{3.2}$$

where γ is the mean ionic activity coefficient, K_i is the equilibrium constant, X is the number of moles of acid reacted per 1,000 g of water in the original acid solution, N is the initial acid molality, and

$$\beta = \frac{1000}{1000+9X} \tag{3.3}$$

The two unknowns in these equations are the calcium concentration and X, which represents the fraction of acid that is reacted. While this method provides a means to determine the concentration of unspent acid, it does not include the necessary reaction kinetics parameters or any influence of mass transfer. Another disadvantage of this approach is that the equilibrium constants are calculated from correlations. Using more modern technology and additional work published in literature since 1976, Buijse et al. developed a model for the use of organic acids in carbonate acidizing (Buijse et al. 2004).

Buijse et al. Model

This work begins with the kinetic rate expression for the reaction of a strong acid, such as HCl:

$$R_{KIN} = k \cdot [H^+]_s^n \tag{3.4}$$

where R_{KIN} is the kinetic rate, k is the reaction rate constant, $[H^+]_s$ is the concentration of H^+ at the mineral surface, and n is the reaction order. As was mentioned previously, the reaction of an organic acid with carbonates occurs in three steps, with the first step being the transport of reactants to the surface. The rate of this mass transport step was given as:

$$R_{MT} = K_{MT}([H^+]_b - [H^+]_s) \quad 3.5$$

where R_{MT} is the rate of mass transport, K_{MT} is the mass transfer coefficient, and $[H^+]_b$ and $[H^+]_s$ are the concentration of H^+ in the bulk solution and at the surface, respectively. At steady state, the two steps are equal. Equating Eq. 3.4 and 3.5, assuming a first order reaction, and solving for $[H^+]_s$, the expression for overall spending rate was given as:

$$R = \frac{k \cdot K_{MT}}{k + K_{MT}} [H^+]_b \quad 3.6$$

For an organic acid, which will not dissociate completely, the correct mass transport rate should be written as:

$$R_{MT} = K_{MT}(C_b - C_s) \quad 3.7$$

where C_b and C_s are the bulk and surface concentrations of the undissociated acid. Buijse et al. stated that organic acids are not dissociated in the bulk solution, but at the surface instead. As H^+ is consumed in the reaction, the acid dissociation reaction progresses towards the dissociated form of the acid. For organic acids, it is necessary to include the acid dissociation constant, K_A, in the calculations. In the Buijse et al. Model, this constant is present within the relationship between C_s and $[H^+]_s$:

$$C_s = [H^+]_s + [HA]_s = [H^+]_s + \frac{[H^+]_s \cdot C_0}{[H^+]_s + K_A} \quad 3.8$$

Assuming a first order reaction at steady state and completely unspent acid, the mass transport and surface reaction rates can again be equated, resulting in:

$$R \cdot \left(1 + \frac{R}{k \cdot K_A}\right) = \frac{k \cdot K_{MT}}{k + K_{MT}} C_0 \quad 3.9$$

Accounting for the incomplete spending of organic acids, the reverse reaction was included in the kinetic rate expression:

$$R_{KIN} = k \cdot \left([H^+]_s^n - \mathrm{X}^n \cdot \frac{(C_0 - C_s)^{2n}}{[H^+]_s^n} \right) \qquad 3.10$$

where X is a relationship between equilibrium constants of the carbonic acid reactions and the solubility product of calcium carbonate.

This model was shown to fit experimental data to a reasonable degree, but several points of concern are present. First, it is assumed that no acid dissociation takes place in the bulk solution, meaning no H^+ is transported to the surface. Although the dissociation constants of typical organic acids are very small compared to HCl, these organic acids will undergo slight dissociation in solution. As a result, the relevant species for the mass transport from the bulk solution to the surface should be both the undissociated acid and the H^+ ion. A second point of concern centers on the authors' statement that the backward reaction term in the final kinetic rate equation is only important for pH > 4, and that this term has a negligible contribution at pH < 4. While this may be true, the pH at the surface of the reacting mineral will be greater than 4, as will be shown in the subsequent model development section. A detailed analysis of the chemistry at the surface of the reacting mineral is necessary to provide a more complete understanding of the overall dissolution process enacted by organic acids on carbonate minerals. Based on these considerations, a third approach to understanding the reaction of organic acids on carbonates was chosen, that of Fredd and Fogler from their investigation of the reaction of acetic acid and calcite (Fredd and Fogler 1998).

A model was developed following the procedure of Fredd and Fogler for acetic acid (Fredd and Fogler 1998). This model calculates the following kinetic parameters: surface reaction rate constant, overall reaction rate constant, effective equilibrium

constant, and the contributions of mass transfer and the surface reaction to overall resistance. The model will be applied for the reaction of lactic acid and calcite, which allows for a thorough investigation of the kinetic parameters of lactic acid.

Due to the reversible nature of reactions involving organic acids, the overall reaction was divided into three steps: the transport of reactants from the bulk solution to the disk surface, the reversible reaction on the disk surface, and the transport of products away from the disk surface. To simplify the mass transfer steps, individual chemical species were grouped together based on similar mass transfer properties. All chemical species classified as reactants were grouped together, all calcium products were grouped together, and all carbonate products were also grouped together, resulting in three separate groups, and the following terms:

$$(H) = (H^+) + (HL) \tag{3.11}$$

$$(M) = (Ca^{2+}) + (CaL^+) + \left(CaHCO_3{}^+\right) + (CaOH^+) \tag{3.12}$$

$$(CO) = (HCO_3{}^-) + \left(CO_3{}^{2-}\right) + (CO_2) + (H_2CO_3) \tag{3.13}$$

where concentrations in Eqs. 3.11-3.13 refer to interface concentrations

Based on the grouped concentration terms, the general reaction equation can be written as:

$$(H) + CaCO_3 \rightleftharpoons (M) + (CO) \tag{3.14}$$

A conditional equilibrium constant can be written based on this general reaction:

$$K_c = \frac{(M)(CO)}{(H)} \tag{3.15}$$

The carbonate concentration at the disk surface has been shown to be independent of disk rotational speed, and can be considered constant (Fredd 1998). Based on this consideration, an effective equilibrium constant can be written as:

$$K_{eff} = \frac{K_c}{(CO)} = \frac{(M)}{(H)} \tag{3.16}$$

The foundation of this model is Eq. 2.1, which can be rearranged and written for each of the three grouped concentration terms.

$$(H) = (H)_b - \frac{r_D}{K_{mt}} \tag{3.17}$$

$$(M) = (M)_b + \frac{r_D}{K_{mt}} \tag{3.18}$$

$$(CO) = (CO)_b + \frac{r_D}{K_{mt}} \tag{3.19}$$

Also, in the mass transfer limited regime, the flux is equal to the dissolution rate. This regime is shown as the linearly increasing portions corresponding to low rotation speeds in **Fig. 3.1**. As disk rotation speed increases, the dissolution rate increases linearly with respect to the square root of the rotation speed. Alternatively, the surface-reaction-limited regime is shown by the horizontal sections corresponding to high rotation speeds in **Fig. 3.1**. This regime can also be shown in **Fig. 3.2**, where the data points from

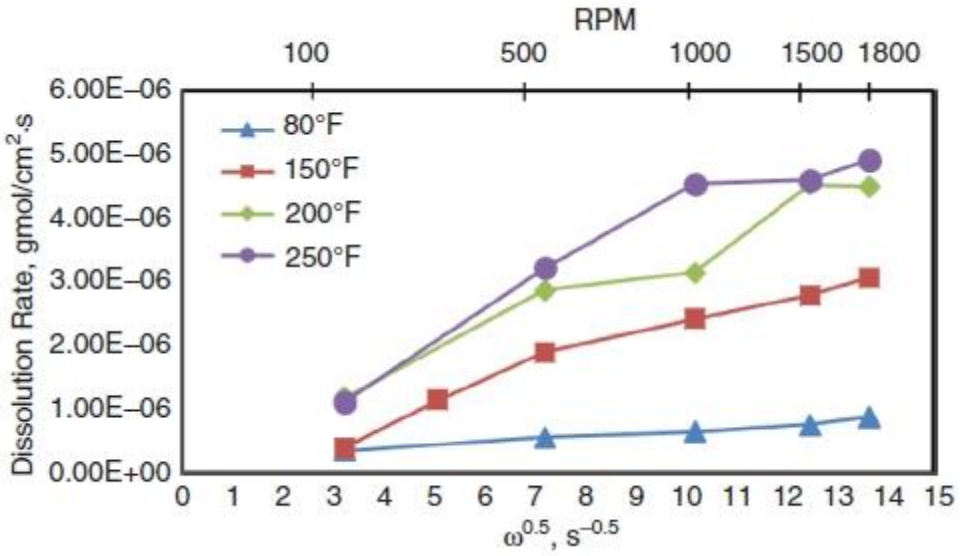

Figure 3.1 – Reaction of 5 wt% lactic acid with Indiana limestone from 80-250°F.

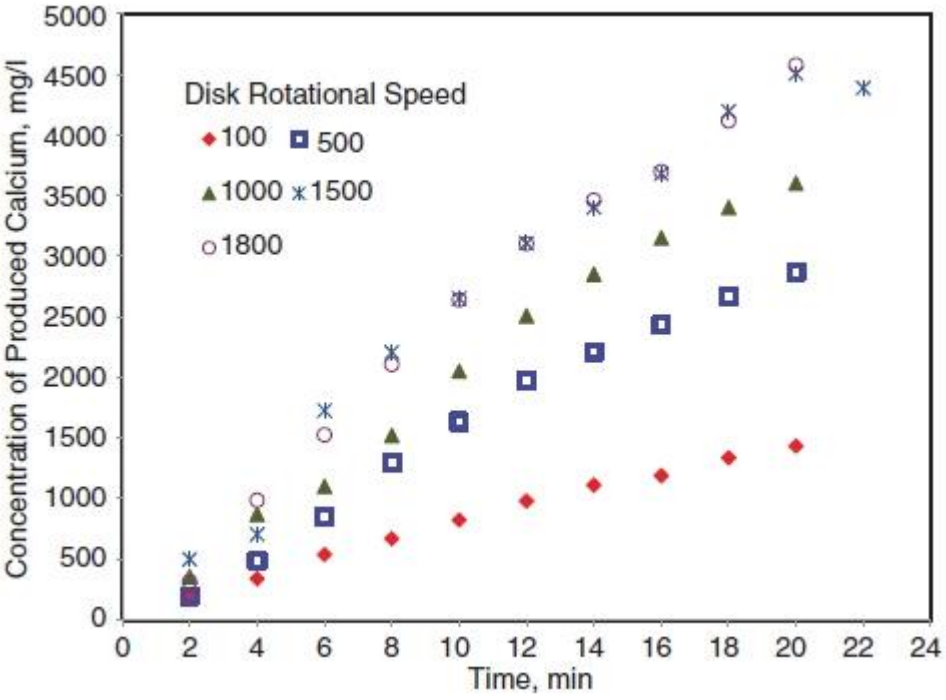

Figure 3.2 – Reaction of 5 wt% lactic acid with Indiana limestone at 200°F.

experiments at 1500 and 1800 RPM are overlapping. This shows that the dissolution rate is no longer limited by mass transfer and is constant above a certain rotation speed. This clear distinction allows for the analysis of each of the two regimes independently by looking only at data corresponding to very low or very high rotation speeds. This allows the experimental dissolution rate values determined from low rotational speed rotating disk experiments to be substituted into the flux equation. Dissolution rates were calculated using only the first several data points obtained from rotating disk experiments. As the reaction progresses, the disk surface can be altered, which would result in an incorrect value for the dissolution rate. This also allows for the substitution of the initial bulk concentrations into the flux equation, as the amounts of reactants consumed and products generated at early time can be considered negligible. The disk rotational speed is known for each experiment, which leaves only the fluid properties and the interface concentrations as unknowns. The kinematic viscosity of lactic acid was measured over a temperature range of 75-176°F, and these values were extrapolated to higher temperatures. The obtained values are listed in **Table 3.1** and shown in **Fig. 3.3**.

80°F	9.463×10^{-3}
150°F	4.637×10^{-3}
250°F	2.859×10^{-3}

Table 3.1 – Kinematic viscosity (cm^2/sec) of 5 wt% lactic acid.

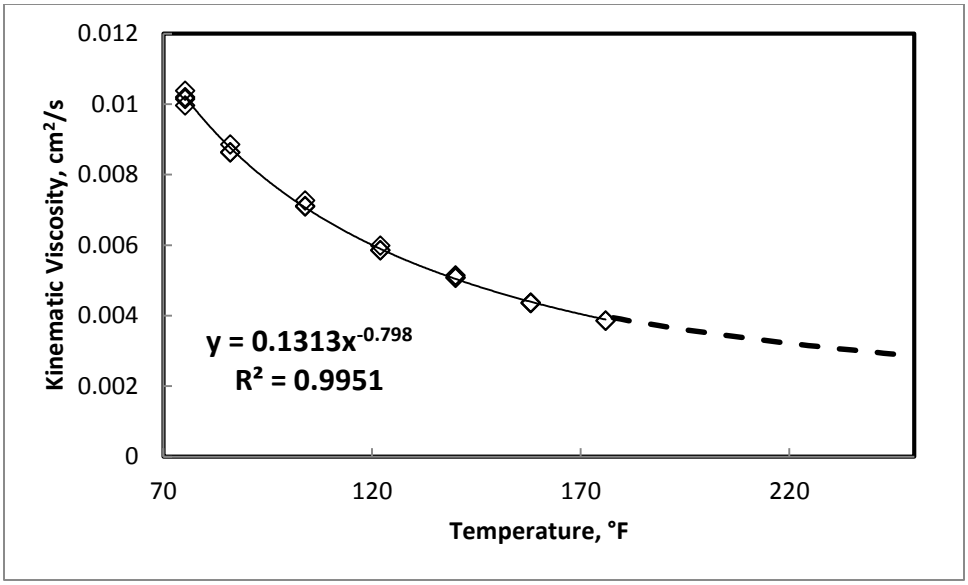

Figure 3.3 – Kinematic viscosity of 5 wt% lactic acid as a function of temperature.

The diffusion coefficient of 5 wt% lactic acid was estimated at 25°C following the procedure of Ribeiro et al. (Ribeiro et al. 2005). The diffusion coefficients of both calcium and carbonate products at 25°C were taken from the assumptions of Fredd and Fogler (Fredd and Fogler 1998). All diffusion coefficients corresponding to higher temperatures were calculated using the estimated values at 25°C and the Arrhenius equation (Levich 1962):

$$D = D_o e^{\frac{-E_a}{kT}} \qquad 3.20$$

All diffusion coefficients used in the model are given in **Table 3.2**. Once the diffusion coefficients were determined, only the interface concentrations of each of the grouped species terms remained as unknowns.

Temperature (°F)	Lactic Acid	Calcium Products	Carbonate Products
80	8.289×10^{-6}	9×10^{-6}	1×10^{-5}
150	1.79×10^{-5}	1.95×10^{-5}	2.16×10^{-5}
250	4.11×10^{-5}	4.46×10^{-5}	4.96×10^{-5}

Table 3.2 – Diffusion coefficients (cm^2/s) used in model calculations.

Another benefit of using data in the mass transfer limited regime is that all species can be assumed to reach equilibrium at the disk surface. The surface reaction is considered rapid compared to the rate of mass transfer towards and away from the disk surface. The complete set of equilibrium equations, along with their corresponding equilibrium constants are given in **Table 3.3**.

Equilibrium Reactions	log *K* (25°C)
$HL \rightleftharpoons H^+ + L^-$	−3.86
$CaL^+ \rightleftharpoons Ca^{2+} + L^-$	−1.47
$CaCO_3 \rightleftharpoons Ca^{2+} + CO_3^{2-}$	−8.34
$CaHCO_3^+ \rightleftharpoons Ca^{2+} + HCO_3^-$	−1.02
$CaOH^+ \rightleftharpoons Ca^{2+} + OH^-$	−1.40
$CaCO_3^\circ \rightleftharpoons Ca^{2+} + CO_3^{2-}$	3.26
$H_2O \rightleftharpoons H^+ + OH^-$	−14.00
$H_2O + CO_2 \rightleftharpoons HCO_3^- + H^+$	−6.37
$H_2CO_3^\circ \rightleftharpoons HCO_3^- + H^+$	−6.37
$HCO_3^- \rightleftharpoons CO_3^{2-} + H^+$	−10.33

Table 3.3 – Equilibrium reactions for calcite/lactic acid system and corresponding equilibrium constants at 25°C (Davies 1962; Dean 1992; Fredd and Fogler 1998).

These equilibrium equations, along with Eqs. 3.12-3.14, are solved simultaneously, resulting in the interface concentrations for all species. Equilibrium constants were corrected using activity coefficients calculated from the extended form of the Debye-Hückel equation, which closely approximates activity coefficients in solutions up to one molal (Robinson and Stokes 1955):

$$\log \gamma = \frac{-Az^2\sqrt{I}}{1+Ba\sqrt{I}} + bI \qquad 3.21$$

where A and B are constants depending on the solvent, z is the ionic charge, I is the ionic strength, a is the "hydrated ion size", and the b parameter allows for the decrease in solvent concentration in concentrated solutions. The values for A, B, a, and b are listed in **Table**s **3.4-3.5**. Equilibrium constants were also corrected for temperature using the Arrhenius equation.

Temperature	A-parameter	B-parameter
80°F	0.5125	0.3294
150°F	0.5558	0.3384
250°F	0.6316	0.3466

Table 3.4 – Values of A and B constants for water (Dean 1992).

Once this set of nonlinear algebraic equations was solved, a value for the effective equilibrium constant, K_{eff}, could be evaluated. The calculated K_{eff} values are shown in **Table 3.6**. This value was then compared with an effective equilibrium constant calculated directly from experimental data.

Species	a-parameter	b-parameter
H^+	9	0
L^-	4.5	0
Ca^{2+}	6	0.165
CaL^+	4.4	0
CO_3^{2-}	4.5	0
HCO_3^-	4	0
$CaHCO_3^+$	4.4	0
OH^-	3.5	0
$CaOH^+$	4.4	0

Table 3.5 – Values of a and b parameters for each ionic species (Truesdell and Jones 1974).

Temperature, °F	K_{eff}
80	0.525
150	0.571
250	0.540

Table 3.6 – Effective equilibrium constants calculated from model.

CHAPTER IV

EXPERIMENTAL RESULTS AND ANALYSIS

Rotating disk experiments were conducted on Indiana limestone disks over a wide range of rotational speeds (100-1800 rpm) and temperatures (80-250°F), with initial acid concentrations corresponding to 1, 5, and 10 wt%. Experiments were also conducted on Silurian dolomite disks at 1500 rpm over a range of temperatures from 80 to 250°F and from 150 to 1800 rpm at 150°F. The complete set of experimental data has been given in the Appendix , and the reproducibility of the data has been shown in **Fig. 4.1**. Although only calcite experiments at 5 wt% lactic acid were used, all experiments showed good repeatability.

The dissolution rate of 5 wt% lactic acid with calcite was calculated from experimental data from 100-1800 rpm and 80-250°F, and was shown previously in **Fig. 3.1**. From this plot, the limiting regime for each set of conditions can be observed. At 80°F, only a very weak dependence on rotational speed is exhibited, so it is apparent that the reaction is mainly limited by the kinetics of the surface reaction at this temperature. As the temperature is increased to 150°F, it is observed that the reaction is limited by mass transfer up to 500 rpm, after which the kinetics of the surface reaction begin to influence the overall reaction. This changed is noted by the distinct change in the slope of the data from **Fig. 3.1**. At 200°F, the overall reaction was limited by mass transfer up to 1500 rpm, but was limited by the surface reaction after 1500 rpm. At 250°F, the

overall reaction was limited by mass transfer up to 1000 rpm, but was surface-reaction-limited after 1000 rpm.

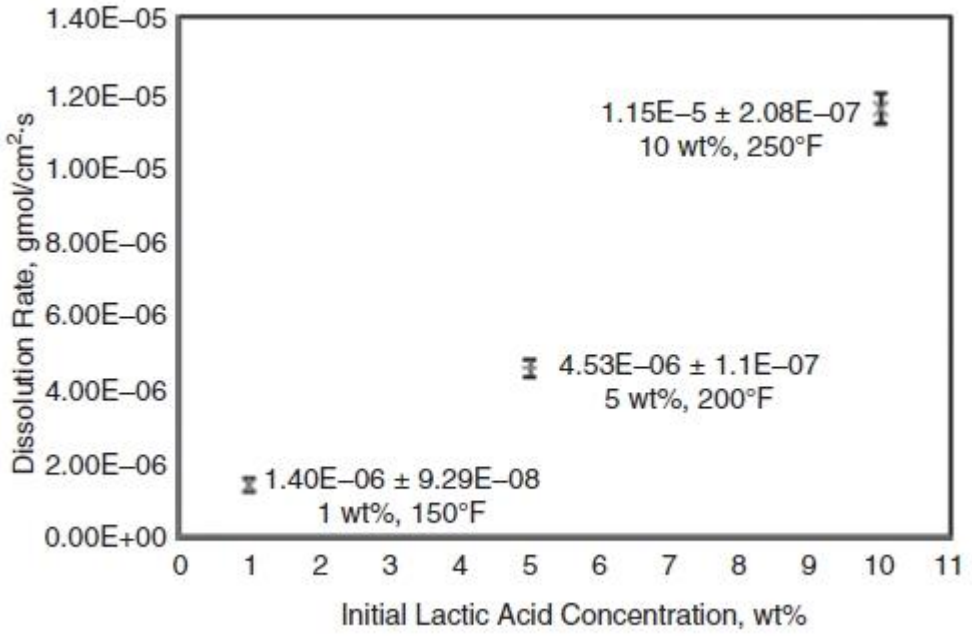

Figure 4.1 – Data Reproducibility at 1500 rpm for the reaction of lactic acid with Indiana limestone.

Mass Transfer Study – Reaction of Lactic Acid with Calcite

The effect of the reversible reaction can be quantified by calculating the activation energy for the reaction of lactic acid with calcite. This can be done by plotting the natural log of the diffusion coefficient versus the reciprocal of the absolute temperature, which is shown in **Fig. 4.2**, and using the slope to calculate the activation energy. It is important to note that the diffusion coefficients used in this case are calculated from the experimental data instead of being estimated as the values used in

the model. These values are calculated using Eq. 2.1, but it is also important to note that this calculation requires the assumption of a negligible reactant concentration at the fluid-mineral interface. The diffusion coefficients, which are present within the Schmidt number in Eq. 2.1, were equal to 5.92×10^{-7}, 9.74×10^{-6}, 1.09×10^{-5}, and 1.47×10^{-5} cm^2/s at 80, 150, 200, and 250°F, respectively. While this assumption is likely valid for a strong acid that dissociates completely, this will not be the case for organic acids.

The Arrhenius equation (Eq. 3.20) was used in order to calculate the activation energy, and a value of 8.41 kcal/mol was obtained. For a purely diffusion-limited reaction, one would expect the activation energy to be approximately 3.8-3.9 kcal/mol. This expectation is based on the measured activation energies for the diffusion of undissociated acetic acid and the viscous flow of water (Vitagliano and Lyons 1956). The difference between the calculated and expected values represents the effect of the reversible reaction. Due to the large magnitude of the difference between the calculated and expected values, it is absolutely necessary to consider this thermodynamic limitation in any reaction kinetics analysis.

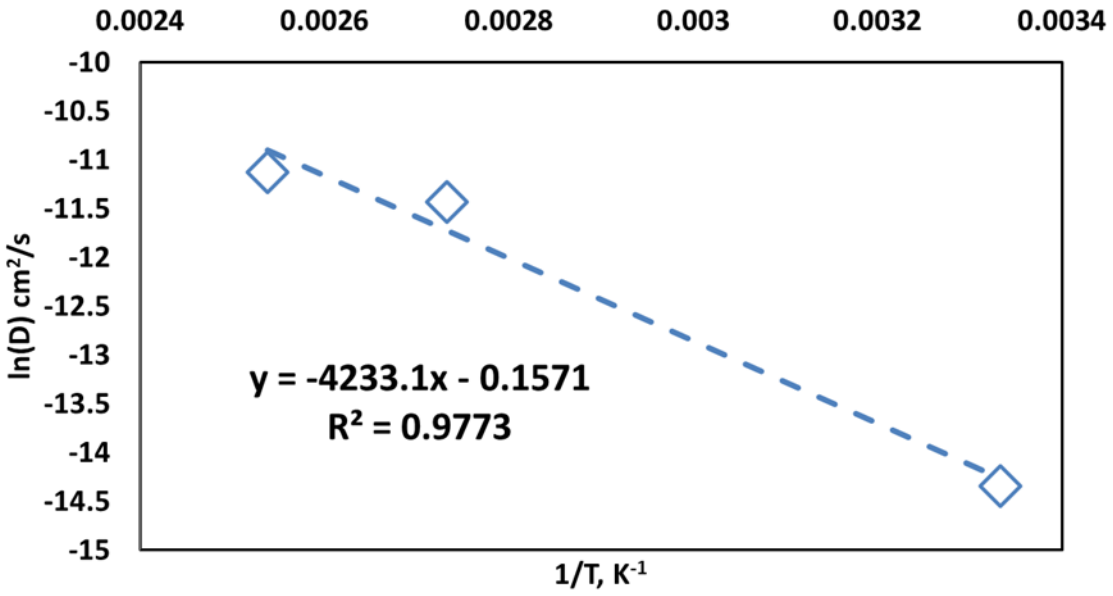

Figure 4.2 – Calculated diffusion coefficients of 5 wt% lactic acid versus temperature.

A similar result was obtained for the reaction of acetic acid with calcite (Fredd and Fogler 1998). This indicates that even at low rotational speeds, there is a thermodynamic limitation on the reaction rate of organic acids with calcite. This is due to the reversible nature of the reaction of organic acids, meaning the reaction is thermodynamically limited by the presence of reaction products. As a result, an accurate diffusion coefficient cannot be calculated for lactic acid due to the non-negligible reactant concentration at the surface. For a strong acid such as HCl, which dissociates completely, the surface concentration of reactants can be assumed to be negligible. Conversely, this assumption cannot be made for the reaction of organic acids with calcite. Instead of dissociating completely, an equilibrium is reached between all species present in the system.

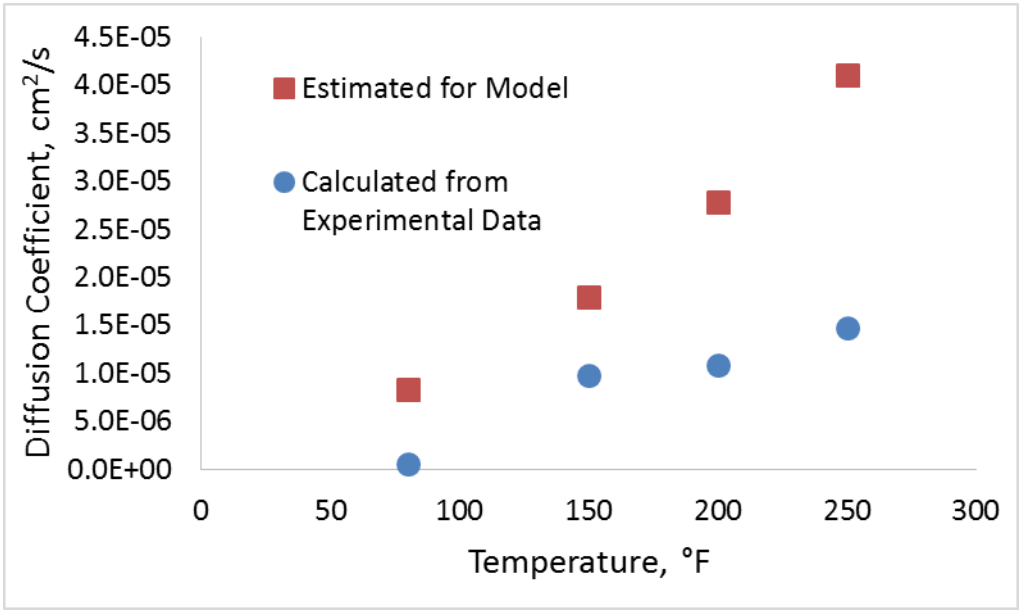

Figure 4.3 – Comparison of estimated and calculated diffusion coefficient values.

The effect of the reversible reaction can be seen in **Fig. 4.3**, as the calculated diffusion coefficients are significantly lower than the estimated values. The estimated values followed a method that closely matched diffusion coefficients measured using Taylor dispersion equipment (Ribeiro et al. 2005), which results in greater accuracy compared to the values calculated from rotating disk data. As has been shown, the reversible nature of the reaction of organic acids with calcite is a major consideration that must not be neglected. This will be further emphasized within the kinetic study.

Kinetic Study – Reaction of Lactic Acid with Calcite

In order to complete the investigation of the reaction of lactic acid with calcite, the kinetics of the reaction were isolated. This was done by using only data points corresponding to the surface-reaction-limited regime at high rotational speeds.

In general, the reaction of a strong acid with calcite can be written as (Alkattan et al. 1998; Al-Khaldi, Nasr-El-Din, and Sarma 2010; Buijse et al. 2004; Lund et al. 1975; Williams 1979):

$$r_s = k(H^+)_s^n \tag{4.1}$$

Where r_s is the surface reaction rate, k is the reaction rate constant, $(H^+)_s$ is the concentration of the hydrogen ion at the surface, and n is the reaction order.

In the case of weak acids, which undergo reversible reactions, the surface reaction rate expression can be written as (Buijse et al. 2004):

$$r_s = k_f(H^+)_s^n - k_b(Ca^{2+})_s^n(HCO_3^-)_s^n \tag{4.2}$$

Where k_f and k_b are the forward and backward reaction rate constants, respectively.

Substituting the grouped concentration terms into the surface reaction rate expression:

$$r_s = k_f(H) - k_b(M)(CO) = k_r\left[(H) - \frac{(M)}{K_{eff}}\right] \tag{4.3}$$

As has been stated previously, the overall reaction of lactic acid with calcite consists of three sequential steps: the transport of reactants from the bulk solution to the disk surface, the reversible reaction on the disk surface, and the transport of reactants away from the disk surface to the bulk solution. At steady state, the rates of all three steps are equal. Equating the expressions of each of the three steps:

$$r_D = \frac{K_{m,r}}{\nu}[(H)_b - (H)] \tag{4.4}$$

$$= k_r\left[(H)_b - \frac{(M)_b}{K_{eff}}\right] \tag{4.5}$$

$$= K_{m,p}[(M) - (M)_b] \quad 4.6$$

Where $K_{m,r}$ and $K_{m,p}$ are the mass transfer coefficients of reactants and products, respectively, ν is the stoichiometric ratio of reactants consumed to products generated, k_r is the effective forward reaction rate constant, and $(C)_b$ concentration terms refer to the bulk concentration of the particular grouped species.

Solving for the interface concentrations in Eqs. 4.4-4.6 and substituting them back into the equations, the overall reaction rate expression can now be written as:

$$r_D = \kappa \left[(H)_b - \frac{(M)_b}{K_{eff}}\right] \quad 4.7$$

where κ is the overall reaction rate constant, as follows:

$$\kappa = \frac{1}{\left(\frac{\nu}{K_{m,r}} + \frac{1}{k_r} + \frac{1}{K_{m,p}K_{eff}}\right)} \quad 4.8$$

A linearized form of Eq. 4.7 (Fredd and Fogler 1998) can be used to determine both K_{eff} and k_r from experimental data. This is done by plotting the reciprocal of the dissolution rate versus the reciprocal of the square root of the rotational speed.

$$\frac{1}{r_D} = \frac{1}{k_f\left[(H)_b - \frac{(M)_b}{K_{eff}}\right]} + \frac{\left[\frac{\nu}{K^*_{m,r}} + \frac{1}{K_{eff}K^*_{m,p}}\right]}{\left[(H)_b - \frac{(M)_b}{K_{eff}}\right]} \frac{1}{\omega^{1/2}} \quad 4.9$$

where $K_i^* = K_i / \omega^{1/2}$

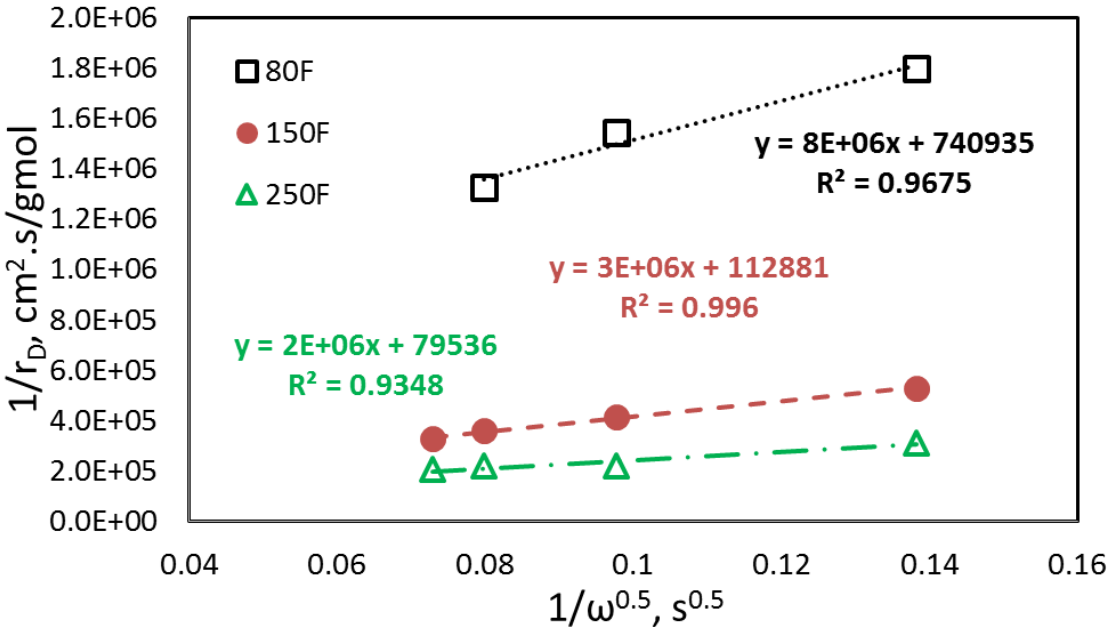

Figure 4.4 – Reciprocal dissolution rate versus reciprocal of the square root of rotational speed for 5 wt% lactic acid at 80, 150, and 250°F.

Using the slope and intercept of the data from **Fig. 4.4**, the effective equilibrium constant and reaction rate constant can be calculated at each temperature. A least squares fit was used to determine each of these parameters, which can be used with Eq. 4.8 to determine the contribution of each step to the overall resistance of the reaction. This is determined by the ratio of each term in the denominator of Eq. 4.8 to the reciprocal of the overall rate constant, κ. Values for K_{eff}, k_r, and the contribution of each step to overall resistance are given in **Table 4.1**.

T (°F)	k_f (cm/s)	K_{eff} Experimental	K_{eff} Model	Reactant Transport	Surface Reaction	Product Transport
80	1.82×10^{-3}	0.537	0.525	22%	28%	50%
150	1.41×10^{-2}	0.579	0.571	28%	13%	59%
250	2.38×10^{-2}	0.607	0.540	30%	10%	60%

Table 4.1 – Reaction kinetics and mass transfer properties of lactic acid with Indiana limestone from 80-250°F.

Values for the effective equilibrium constant determined directly from experimental data differed from the values determined using the model by less than 3% at 80 and 150°F, and by less than 12% at 250°F. There are several potential causes for the higher error at higher temperature. The kinematic viscosity was only measured directly for the first two temperatures, whereas it was calculated using a correlation at 250°F based on the values measured at lower temperatures. Also, the diffusion coefficients were estimated at all temperatures. **Fig. 4.5** shows a comparison of the calculated and model K_{eff} values in addition to the reaction rate constant at all three temperatures.

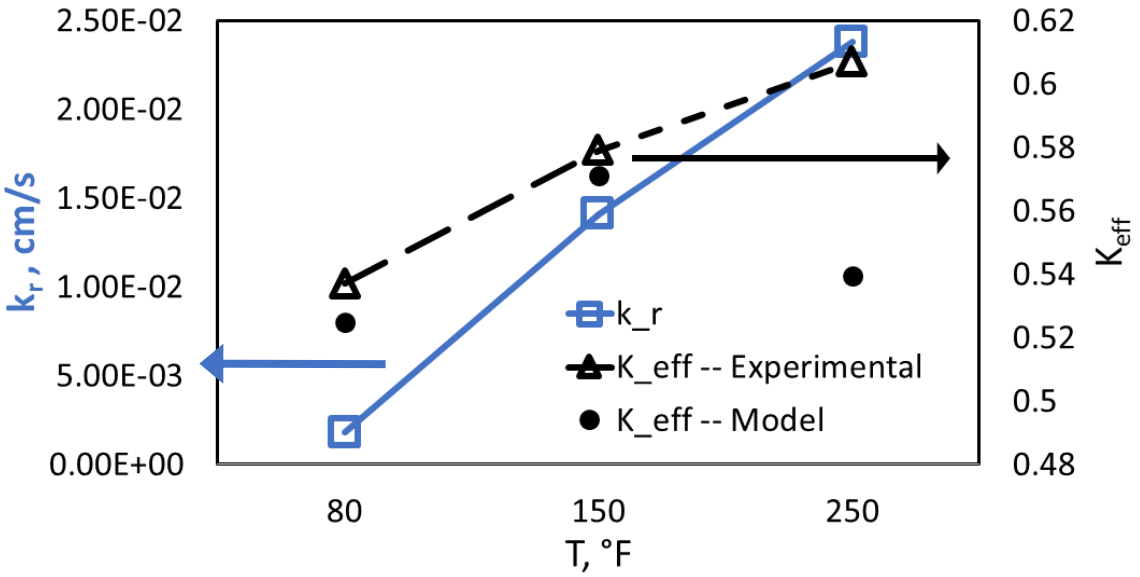

Figure 4.5 – Comparison of experimental and model K_{eff} values and k_r.

The contribution of each step, shown in **Table 4.1** and **Fig. 4.6**, enable the rate-limiting step to be determined. It is important to note that the transport of products from the disk surface back to the bulk solution represented the largest portion of the overall resistance at all investigated temperatures. Much of the previously-published work regarding the reaction of organic acids with carbonates has neglected the effect of the reversible reaction. Based on the findings in this work, this effect must be considered. It can also be noted that the resistance from the surface reaction, although decreasing with increasing temperature, still comprises 10% of the overall resistance at 250°F. As temperature increases, the two mass transfer steps become more limiting.

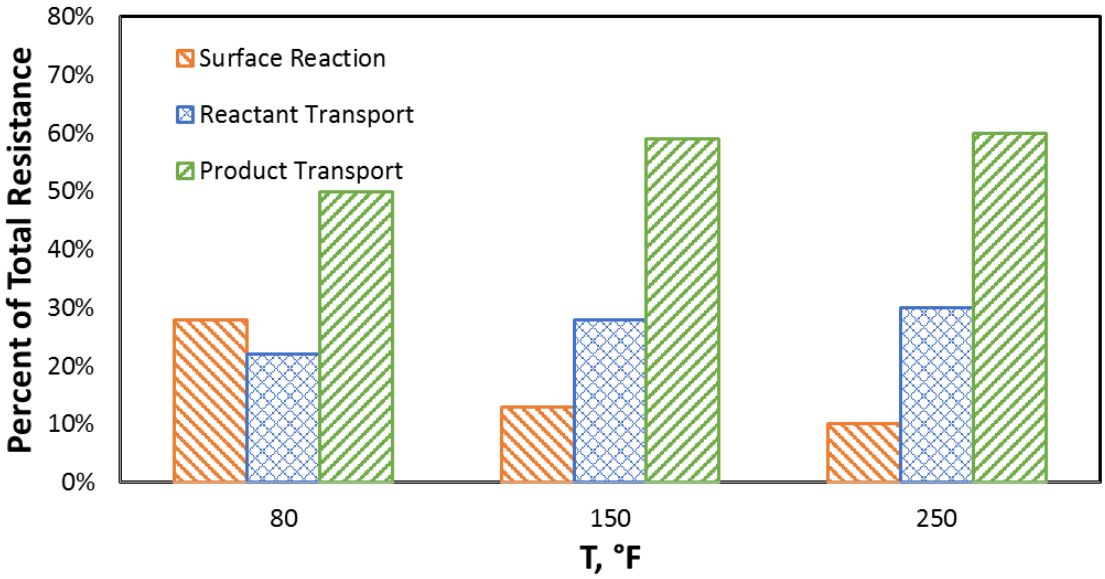

Figure 4.6 – Effect of Temperature on Kinetics.

The necessity of including the influence of the reversible reaction can further be shown by calculating and comparing the values of the reaction rate constant with and without the influence of the reversible reaction. Previous work on lactic acid neglected the influence of the reversible reaction, so the published values for the reaction rate constant were compared with the reaction rate constants calculated in this current work (Rabie and Nasr-El-Din 2011). This comparison is shown in **Table 4.2**. Neglecting the concentration of reactants at the interface resulted in an underestimation of the reaction rate constant. This is as expected based on Eq. 2.1, as this assumption results in an overestimation of the concentration gradient. In order to match the experimentally-determined dissolution rate values, the calculated rate constant will be lower than the actual reaction rate constant.

T, °F	k_r with reversible reaction, cm/s (this study)	k_r without reversible reaction, cm/s (Rabie and Nasr-El-Din 2011)
80	1.82E-03	3.83E-04
150	1.41E-02	1.63E-03
250	2.38E-02	1.05E-03

Table 4.2 – Effect of reversible reaction on calculation of reaction rate constant.

CHAPTER V

COREFLOOD INVESTIGATION

After the necessary kinetic parameters were determined, the next step was to show that lactic acid exhibited wormholing tendencies when injected into calcite cores. This was done using a coreflood test, and a schematic of the equipment is shown in **Fig. 5.1**.

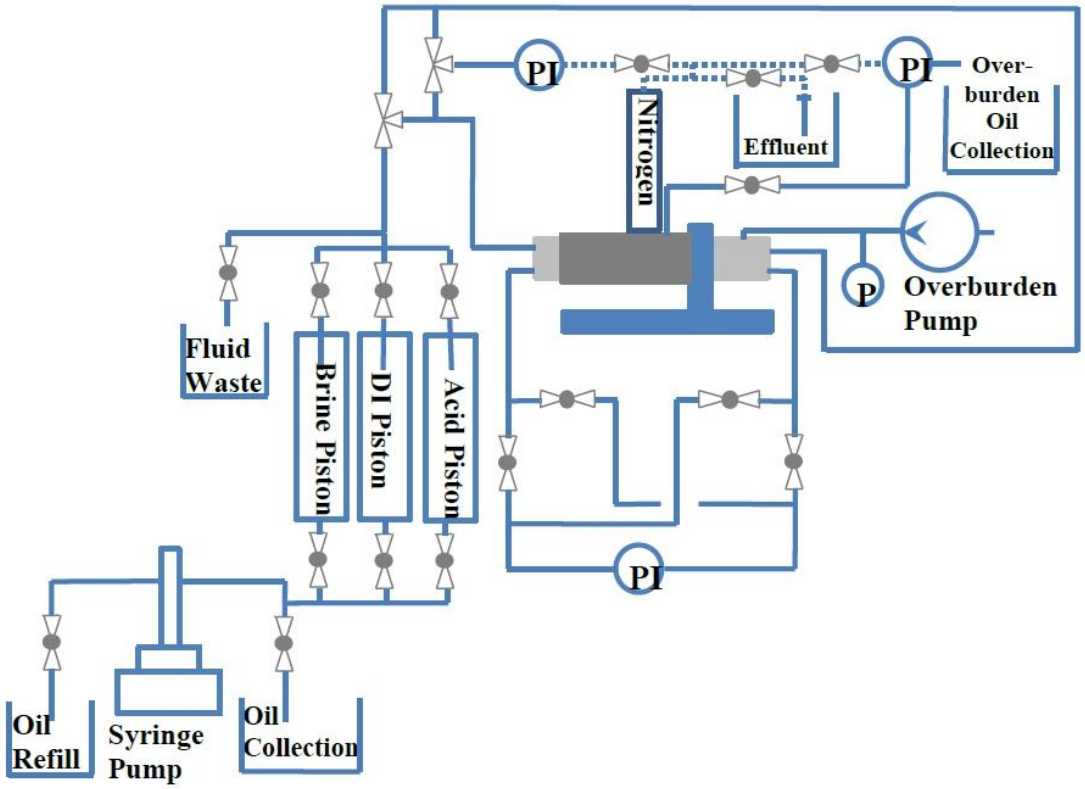

Figure 5.1 – Schematic of coreflood apparatus (Arensman 2014).

The coreflood apparatus consists of a syringe pump that pumps a fluid (either acid, deionized water, or brine) at a constant flow rate through the core, which is housed in a core holder. The core holder contains an overburden sleeve, which allows overburden pressure to be applied, and a heating jacket, which allows experiments to be conducted up to 325°F. The overburden sleeve is necessary to ensure that all fluid flows through the core instead of around the core. Once the fluid passes through the core, effluent samples are collected and analyzed. A pressure transducer measures the pressure drop across the core during fluid injection, and this data is recorded. A backpressure regulator is also in place, which allows the pressure in the core to be held at a value high enough to keep all generated CO_2 in solution.

In order to show the wormholing tendencies of lactic acid in calcite, one coreflood experiment was performed by pumping a 10 wt% lactic acid solution that included 0.1 vol% of a corrosion inhibitor for organic acids through an Indiana limestone core with dimensions of 6 in. length and 1.5 in. diameter.

Before the coreflood experiment was performed, the porosity and permeability of the core were measured. In order to measure the porosity of the core, it was dried in an oven for four hours at 250°F, and the weight of the dried core was recorded. Next, the core was saturated under vacuum in deionized water for three hours. To ensure complete saturation of the core, the initial permeability was measured next. For this step, the overburden pressure was set to 2,000 psi and no backpressure was applied. Deionized water was injected through the core at several low flow rates. The permeability of the core can then be calculated from the pressure drop corresponding to these flow rates.

The core was then weighed to determine its water-saturated weight. The difference between the dry and saturated weight was then used to calculate the porosity of the core. The core that was used had an initial porosity of 16.7 vol% and an initial permeability of 13.2 md.

Before acid injection was started, deionized water was injected through the core, and the heating jacket was set to 250°F. Water was continuously injected until the temperature and pressure drop across the core had both stabilized. Then, the 10 wt% lactic acid solution was injected at a flow rate of 0.5 mL/min until acid breakthrough occurred. Once the wormhole has propagated through the entire length of the core, the pressure drop will be negligible. **Fig. 5.2** shows the pressure drop profile of this experiment. It can be seen that for this experiment, approximately 1.8 pore volumes (49 mL) of acid were required to achieve breakthrough.

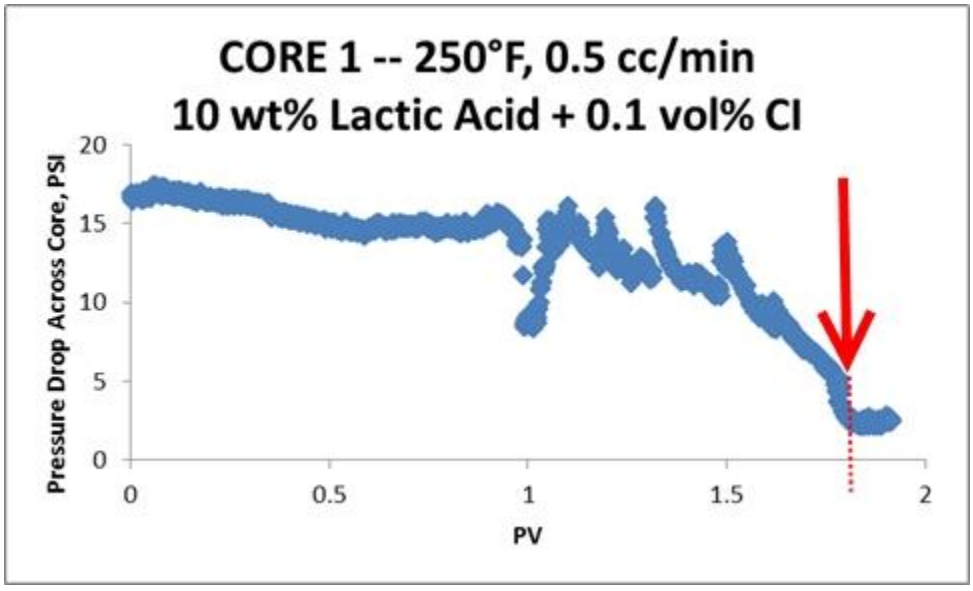

Figure 5.2 – Pressure drop data during acid injection.

Once breakthrough was achieved, deionized water was again injected through the core to remove any unreacted acid, and the core was again dried in an oven. The next step was to determine how the wormhole propagated through the core, which was done using a CT scanner. This results from the CT scan are shown in **Fig. 5.3**, which shows minimal branching and a moderate wormhole diameter.

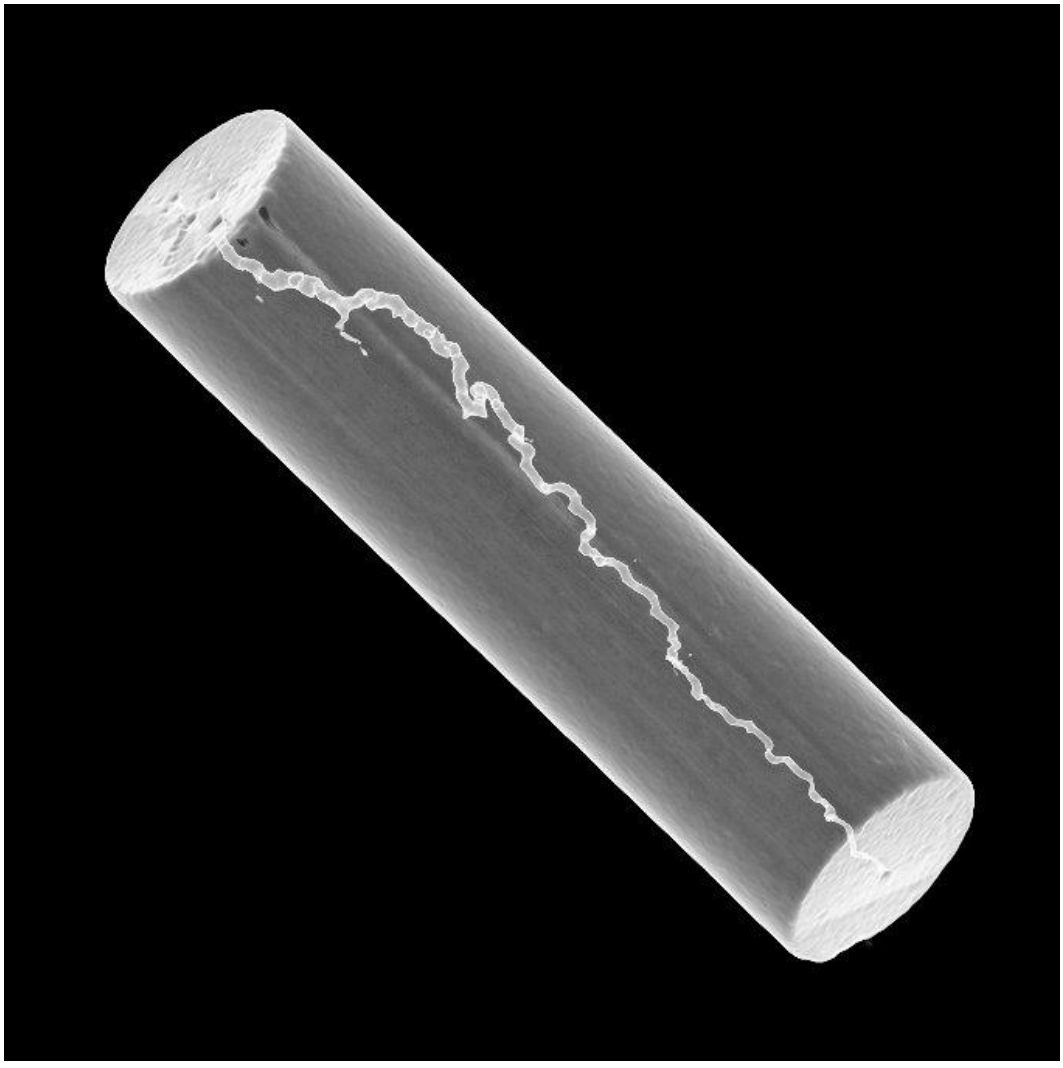

Figure 5.3 – CT scan image of core after acid injection.

For both coreflood experiments and matrix acidizing treatments in the field, the optimum injection rate is signified by the injection rate for which a minimum amount of acid is required for a given increase in productivity. For coreflood experiments, a calculation of the minimum pore volumes to breakthrough can be used to determine the optimum injection rate. This corresponds to the minimum volume of acid required for a wormhole to propagate from the inlet to the outlet of the core. While the optimum injection rate cannot be determined from one coreflood experiment at one injection rate, the injection rate chosen (0.5 mL/min) is near the optimum rate. The single dominant, minimally-branched wormhole is evidence of this.

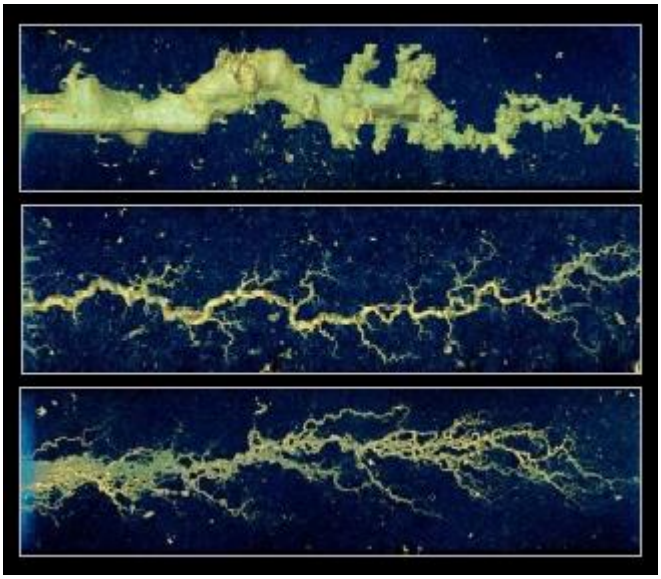

Figure 5.4 – The effect of injection rate on wormhole geometry (McDuff et al. 2010).

The general effect of injection rate on the geometry of the wormholes that are formed is shown in **Fig. 5.4** (McDuff et al. 2010), where injection rate increases from top to bottom, with the middle being the optimum injection rate. As injection rate decreases, the diameter of the wormhole will increase due to an increased residence time, especially at the inlet face of the core. This leads to the formation of conical wormholes or face dissolution at extremely low flow rates. Face dissolution occurs when most of the acid reacts on the face of the core, which leads to a large portion of the core being dissolved without significantly increasing permeability. At flow rates above the optimum rate, the single wormhole will become branched. Branching will also lead to an increase in acid consumption before breakthrough is achieved.

CHAPTER VI

APPLICATION AND CONCLUSIONS

Due to its rapid reaction and high rate of corrosion, there is a need for an alternative to HCl in high-temperature matrix acidizing environments or with acid-sensitive metallurgy. This alternative should have a lower reaction rate and a corrosion rate that can be inhibited. Several organic acids meet these conditions and are readily available. Acetic, formic, and citric acids are commonly used organic acids, but they are not without drawbacks and limitations. First, the dissociation constant of acetic acid is low compared formic acid. Formic acid is not environmentally friendly. Finally, the solubility of the calcium salts formed during the use of these three organic acids is very limited. For field treatments, acetic acid is typically limited to 13 wt% live acid concentration and formic to 9 wt% live acid concentration. This is to avoid precipitation and potential formation damage due to calcium acetate or calcium formate.

Based on these limitations, lactic acid was chosen for a detailed kinetic investigation. The dissociation constant of lactic acid is approximately ten times greater than acetic acid, and it is similar in strength to formic acid. Lactic acid is also environmentally friendly. The solubility of calcium lactate has been shown to be up to 50 wt% at 176°F (Kubantseva and Hartel 2002). A suitable candidate for high temperature matrix acidizing must also be stable over a wide range of temperatures. Lactic acid is thermally stable up to 375°F (EPA 2009).

Based on the advantages that were presented, a more thorough investigation of lactic acid was deemed necessary. As is the case for all organic acids, the reaction of lactic acid with carbonate minerals is reversible, meaning that the reaction is thermodynamically limited by the presence of products at the solid-liquid interface. To account for this, a kinetic model was developed. The results of this model provided valuable reaction kinetics and mass transfer properties that are needed for the optimization of field treatment design. It was shown that for the reaction of lactic acid with calcite, the reversible reaction must be considered. While the assumption that the reverse reaction term can be neglected at pH < 4 (Buijse et al. 2004) may be correct, the pH at the reacting surface will be greater than this, so it is necessary to account for the reverse reaction.

Due to the reversible reaction, the diffusion coefficient of the lactic acid solution cannot be calculated directly from the experimental data presented here. The calculated diffusion coefficient would represent the transport of all reactants and products at equilibrium instead of the reactants alone. This was shown by calculating an activation energy for the reaction of lactic acid with calcite and comparing it with the expected activation energy for a pure diffusion process, where the calculated value was more than double the expected activation energy.

The kinetic model was also used to isolate the contributions of the transport of reactants, the surface reaction, and the transport of products to the overall resistance of the reaction. At all temperatures investigated, the transport of products away from the surface represented the largest contribution to overall resistance. Product transport was

responsible for 60% of the overall resistance at 250°F. As the temperature increased, the contribution of the surface reaction decreased. As the surface reaction rate increased, the transport of reactants to the surface began to limit the reaction to a higher degree, although never more than half as great as the contribution of the transport of products.

Once a thorough kinetic analysis was done and a better understanding of the reaction of lactic acid with calcite was obtained, a coreflood experiment was performed to investigate the wormholing behavior of lactic acid in Indiana limestone cores. Lactic acid formed a single minimally-branched wormhole that propagated from the inlet of the core to the outlet after the injection of 1.8 pore volumes of 10 wt% lactic acid.

CHAPTER VII

FUTURE WORK

Based on the findings presented in this work, further work could provide a more comprehensive understanding of the reaction of lactic acid with calcite. First, a complete set of rotating disk experiments could be performed using 10 wt% lactic acid. Once the dissolution rate values were obtained, the model could be adjusted to obtain the same reaction kinetics and mass transfer properties for this new acid concentration. These properties could then be used for the optimization of additional coreflood experiments. This would allow for the determination of an optimum injection rate. Additionally, coreflood experiments could be conducted at different temperatures, where the optimum injection rate could be determined for each temperature.

REFERENCES

Al-Khaldi, M.H., Nasr-El-Din, H.A., Blauch, M.E. et al. 2005. New Findings on Damage Potential, Geochemical Reaction Mechanisms, and Production Enhancement Applications for Citric Acid. Proc., SPE European Formation Damage Conference, The Hague, Netherlands, 267-275, http://dx.doi.org/10.2118/82218-MS.

Al-Khaldi, M.H., Nasr-El-Din, H.A., Sarma, H. 2010. Kinetics of the Reaction of Citric Acid with Calcite. *SPE J.* **15** (3): 704-713. http://dx.doi.org/10.2118/118724-PA.

Al-Otaibi, M. B., Al-Moajil, A. M., Nasr-El-Din, H. A. 2006. In- Situ Acid System to Clean up Drill-in Fluid Damage in High- Temperature Gas Wells. Proc., IADC/SPE Asia Pacific Drilling Technology Conference and Exhibition, Bangkok, Thailand, http://dx.doi.org/10.2118/103846-MS.

Alkattan, M., Oelkers, E.H., Dandurand, J.L. et al. 1998. An Experimental Study of Calcite and Limestone Dissolution Rates as a Function of Ph from -1 to 3 and Temperature from 25 to 80 Degrees C. *Chem. Geol.* **151** (1-4): 199-214. http://dx.doi.org/10.1016/S0009-2541(98)00080-1.

Arensman, D.G. 2014. Acidizing Dolomite Reservoirs Using Hcl Acid Prepared with Seawater: Problems and Solutions. MS, Texas A&M University, College Station, TX (May 2014).

Bennion, D.B., Thomas, F.B. 1994. Underbalanced Drilling of Horizontal Wells: Does It Really Eliminate Formation Damage? Proc., SPE Intl. Symposium on Formation Damage Control, Lafayette, LA, http://dx.doi.org/10.2118/27352-MS.

Boomer, D.R., McCune, C.C., Fogler, H.S. 1972. Rotating Disk Apparatus for Reaction Rate Studies in Corrosive Liquid Environments. *Review of Scientific Instruments* **43** (2): 225-229. http://dx.doi.org/10.1063/1.1685599.

Buijse, M., de Boer, P., Breukel, B. et al. 2004. Organic Acids in Carbonate Acidizing. *SPE Production and Facilities* **19** (3): 128-134. http://dx.doi.org/10.2118/82211-PA.

Chatelain, J.C., Silberberg, I.H., Schechter, R.S. 1976. Thermodynamic Limitations in Organic-Acid/Carbonate Systems. *SPE J.* **16** (4): 189-195. http://dx.doi.org/10.2118/5647-PA.

Civan, F. 2007. *Reservoir Formation Damage Fundamentals, Modeling, Assessment, and Mitigation*. Amsterdam ; Boston, Gulf Professional Pub. (Reprint). http://dx.doi.org/10.1016/B978-075067738-7/50002-6.

Crowe, C.W., Minor, S.S. 1985. Effect of Acid Corrosion Inhibitors on Matrix Stimulation Results. *Journal of Petroleum Technology* **37** (10): 1853-1860. http://dx.doi.org/10.2118/11119-PA.

Davies, C.W. 1962. *Ion Association*. Washington D.C., Butterworths (Reprint).

Dean, J.A. 1992. *Lange's Handbook of Chemistry*. New York, McGraw-Hill (Reprint).

Ellison, B.T., Cornet, I. 1971. Mass Transfer to a Rotating Disk. *J. Electrochem. Soc.* **118** (1): 68-72. http://dx.doi.org/10.1149/1.2407954.

EPA. 2009. *Biopesticides Registration Action Document L-Lactic Acid*. Washington D.C., BiblioGov (Reprint).

Fredd, C.N. 1998. The Influence of Transport and Reaction on Wormhole Formation in Carbonate Porous Media: A Study of Alternative Stimulation Fluids. Doctor of Philosophy, The University of Michigan.

Fredd, C.N., Fogler, H.S. 1998. The Kinetics of Calcite Dissolution in Acetic Acid Solutions. *Chemical Engineering Science* **53** (22): 3863-3874. http://dx.doi.org/10.1016/S0009-2509(98)00192-4.

Huang, T.P., Hill, A.D., Schechter, R.S. 2000. Reaction Rate and Fluid Loss: The Keys to Wormhole Initiation and Propagation in Carbonate Acidizing. *SPE J.* **5** (3): 287-292. http://dx.doi.org/10.2118/37312-MS.

Kalfayan, L. 2008. *Production Enhancement with Acid Stimulation*. Tulsa, OK, PennWell (Reprint).

Kubantseva, N., Hartel, R.W. 2002. Solubility of Calcium Lactate in Aqueous Solution. *Food Reviews International* **18** (2-3): 135-149. http://dx.doi.org/10.1081/FRI-120014355.

Levich, V.G. 1962. *Physicochemical Hydrodynamics*. Englewood Cliffs, NJ, Prentice-Hall (Reprint).

Li, L., Nasr-El-Din, H.A., Chang, F.F. et al. 2008. Reaction of Simple Organic Acids and Chelating Agents with Calcite. Proc., International Petroleum Technology Conference, Kuala Lumpur, Malaysia, http://dx.doi.org/10.2523/12886-MS.

Lund, K., Fogler, H.S., McCune, C.C. 1973. Acidization— I. The Dissolution of Dolomite in Hydrochloric Acid. *Chemical Engineering Science* **28** (3): 691,IN1-700,IN1. http://dx.doi.org/10.1016/0009-2509(77)80003-1.

Lund, K., Fogler, H.S., McCune, C.C. et al. 1975. Acidization— Ii. The Dissolution of Calcite in Hydrochloric Acid. *Chemical Engineering Science* **30** (8): 825-835. http://dx.doi.org/10.1016/0009-2509(75)80047-9.

McDuff, D.R., Shuchart, C.E., Jackson, S.K. et al. 2010. Understanding Wormholes in Carbonates: Unprecedented Experimental Scale and 3-D Visualization. Proc., SPE Annual Technical Conference and Exhibition, Florence, Italy, http://dx.doi.org/10.2118/134379-MS.

Newman, J. 1966. Schmidt Number Correction for the Rotating Disk. *The Journal of Physical Chemistry* **70** (4): 1327-1328. http://dx.doi.org/10.1021/j100876a509.

Plummer, L.N., Wigley, T.M.L., Parkhurst, D.L. 1978. The Kinetics of Calcite Dissolution in Co_2-Water Systems at 5° to 60°C and 0.0 to 1.0 Atm Co_2. *American Journal of Science* **278** (2): 179-216. http://dx.doi.org/10.2475/ajs.278.2.179.

Pokrovsky, O.S., Golubev, S.V., Schott, J. 2005. Dissolution Kinetics of Calcite, Dolomite and Magnesite at 25 °C and 0 to 50 Atm Pco2. *Chemical Geology* **217** (3–4): 239-255. http://dx.doi.org/10.1016/j.chemgeo.2004.12.012.

Pokrovsky, O.S., Golubev, S.V., Schott, J. et al. 2009. Calcite, Dolomite and Magnesite Dissolution Kinetics in Aqueous Solutions at Acid to Circumneutral Ph, 25 to 150 °C and 1 to 55 atm Pco2: New Constraints on Co2 Sequestration in Sedimentary Basins. *Chemical Geology* **265** (1–2): 20-32. http://dx.doi.org/10.1016/j.chemgeo.2009.01.013.

Rabie, A.I., Nasr-El-Din, H. A. 2011. Measuring the Reaction Rate of Lactic Acid with Calcite Using the Rotating Disk Apparatus. Proc., SPE Middle East Oil and Gas Show and Conference, Manama, Bahrain, http://dx.doi.org/10.2118/140167-ms.

Ribeiro, A.C.F., Lobo, V.M.M., Leaist, D.G. et al. 2005. Binary Diffusion Coefficients for Aqueous Solutions of Lactic Acid. *J. Solut. Chem.* **34** (9): 1009-1016. http://dx.doi.org/10.1007/s10953-005-6987-3.

Robinson, R.A., Stokes, R.H. 1955. *Electrolyte Solutions; the Measurement and Interpretation of Conductance, Chemical Potential and Diffusion in Solutions of Simple Electrolytes*. London, Butterworths Scientific Publications (Reprint).

Schauhoff, S., Kissel, C.L. 2000. New Corrosion Inhibitors for High Temperature Applications. *Materials and Corrosion* **51** (3): 141-146. http://dx.doi.org/10.1002/(SICI)1521-4176(200003)51:3<141::AID-MACO141>3.0.CO;2-N.

Sjöberg, E.L., Rickard, D.T. 1984. Calcite Dissolution Kinetics: Surface Speciation and the Origin of the Variable Ph Dependence. *Chemical Geology* **42** (1-4): 119-136. http://dx.doi.org/10.1016/0009-2541(84)90009-3.

Taylor, K.C., Nasr-El-Din, H.A. 2009. Measurement of Acid Reaction Rates with the Rotating Disk Apparatus. *Journal of Canadian Petroleum Technology* **48** (6): 66-70. http://dx.doi.org/10.2118/09-06-66.

Truesdell, A.H., Jones, B.F. 1974. Wateq, a Computer Program for Calculating Chemical Equilibria of Natural Waters. *Journal of Research of the U.S. Geological Survey* **2** (2): 233-248.

Tuttle, R.N. 1987. Corrosion in Oil and Gas Production. *Journal of Petroleum Technology* **39** (7): 756-762. http://dx.doi.org/10.2118/17004-PA.

Vitagliano, V., Lyons, P.A. 1956. Diffusion in Aqueous Acetic Acid Solutions. *Journal of the American Chemical Society* **78** (18): 4538-4542. http://dx.doi.org/10.1021/ja01599a008.

Williams, B.B. 1979. *Acidizing Fundamentals*. New York, Henry L. Doherty Memorial Fund of AIME, Society of Petroleum Engineers of AIME (Reprint).

APPENDIX

SUMMARY OF EXPERIMENTAL DATA

Run	Initial Acid Concentration (wt%)	Temperature (°F)	Disk Rotational Speed (rev/min)	Rate of Dissolution (g mol/cm^2·s)
C-08	5	80	100	3.46×10^{-7}
C-09	5	80	500	5.57×10^{-7}
C-10	5	80	1,000	6.47×10^{-7}
C-11	5	80	1,500	7.55×10^{-7}
C-12	5	80	1,800	8.69×10^{-7}
C-13	5	80	1,800	8.70×10^{-7}
C-14	5	150	100	3.96×10^{-7}
C-15	5	150	250	1.13×10^{-6}
C-16	5	150	500	1.89×10^{-6}
C-17	5	150	1,000	2.42×10^{-6}
C-18	5	150	1,500	2.78×10^{-6}
C-19	5	150	1,800	3.06×10^{-6}
C-20	5	200	100	1.18×10^{-6}
C-21	5	200	500	2.86×10^{-6}
C-22	5	200	1,000	3.14×10^{-6}
C-23	5	200	1,500	4.42×10^{-6}
C-24	5	200	1,500	4.53×10^{-6}
C-25	5	200	1,500	4.64×10^{-6}
C-26	5	200	1,800	4.50×10^{-6}
C-27	5	250	100	1.11×10^{-6}
C-28	5	250	500	3.21×10^{-6}
C-29	5	250	1,000	4.54×10^{-6}
C-30	5	250	1,500	4.60×10^{-6}
C-31	5	250	1,800	4.91×10^{-6}
C-32	5	300	1,500	5.17×10^{-6}